amontillado, the Drosophila Homolog of the Prohormone Processing Protease PC2, Is Required During Embryogenesis and Early Larval Development

Lowell Y. M. Rayburn,* Holly C. Gooding,*,[1] Semil P. Choksi,*,[2] Dhea Maloney,*,[3] Ambrose R. Kidd, III,*,[4] Daria E. Siekhaus†,[5] and Michael Bender*,[6]

**Department of Genetics, The University of Georgia, Athens, Georgia 30602 and †Department of Biochemistry, Stanford University School of Medicine, Stanford, California 94305*

Manuscript received August 19, 2002
Accepted for publication October 23, 2002

ABSTRACT

Biosynthesis of most peptide hormones and neuropeptides requires proteolytic excision of the active peptide from inactive proprotein precursors, an activity carried out by subtilisin-like proprotein convertases (SPCs) in constitutive or regulated secretory pathways. The Drosophila *amontillado* (*amon*) gene encodes a homolog of the mammalian PC2 protein, an SPC that functions in the regulated secretory pathway in neuroendocrine tissues. We have identified *amon* mutants by isolating ethylmethanesulfonate (EMS)-induced lethal and visible mutations that define two complementation groups in the *amon* interval at 97D1 of the third chromosome. DNA sequencing identified the *amon* complementation group and the DNA sequence change for each of the nine *amon* alleles isolated. *amon* mutants display partial embryonic lethality, are defective in larval growth, and arrest during the first to second instar larval molt. Mutant larvae can be rescued by heat-shock-induced expression of the *amon* protein. Rescued larvae arrest at the subsequent larval molt, suggesting that *amon* is also required for the second to third instar larval molt. Our data indicate that the *amon* proprotein convertase is required during embryogenesis and larval development in Drosophila and support the hypothesis that AMON acts to proteolytically process peptide hormones that regulate hatching, larval growth, and larval ecdysis.

MOST biologically active peptide hormones and neuropeptides are produced from larger inactive precursor proteins by endoproteolytic cleavage and further processing within the secretory pathway (Sossin *et al.* 1989; Rouille *et al.* 1995b; Bergeron *et al.* 2000). Endoproteolytic processing of peptide hormones and other secreted and transmembrane proteins is carried out by a family of serine proteases, the subtilisin-like proprotein convertases (SPCs), that typically cleave precursor proteins after single or paired basic residues (Creemers *et al.* 1998; Seidah *et al.* 1999; Zhou *et al.* 1999). SPCs function in constitutive and regulated secretory pathways in a variety of cell types. Precursor proteins may be cleaved by SPCs to liberate multiple bioactive products (Sossin *et al.* 1989; Zhou *et al.* 1999), and a given precursor may be differentially processed in a cell-specific fashion depending on the SPC processing enzymes expressed (Rouille *et al.* 1995a; Furuta *et al.* 1997).

To date, seven members of the SPC family have been identified in vertebrates (Muller and Lindberg 2000). All of the family members share a common structural organization and are themselves synthesized as inactive propeptides. The N-terminal signal sequence, or Pre domain, is required to target the protein to the secretory pathway and is removed by a signal peptidase once the protein has reached the endoplasmic reticulum. The Pro domain is believed to be an intramolecular chaperone and its removal during enzyme maturation is essential for the protein to become active (Zhu *et al.* 1989). The catalytic domain of the proprotein convertases is the most conserved among family members; vertebrate members display 40–50% homology with subtilisin in this domain, which contains the catalytic triad residues aspartate, histidine, and serine (Rouille *et al.* 1995a). The catalytic domain also contains an oxyanion hole that is essential for catalysis (Bryan *et al.* 1986). Interestingly, in all family members except for prohormone convertase 2 (PC2), this residue is an asparagine. PC2 contains an aspartate at this position. The asparagine or aspartate residue stabilizes the negative charge induced on the carbonyl oxygen of the peptide bond being cleaved (Bryan *et al.* 1986). The P domain influences proper folding of the protein as well as contributes to the calcium dependence, pH requirement, and stability of the convertase (Zhou *et al.* 1998). All family members

[1]*Present address:* University of California-San Francisco/Berkeley Joint Medical Program, Berkeley, CA 94720.

[2]*Present address:* Department of Genetics, University of Cambridge, Cambridge CB2 3EH, UK.

[3]*Present address:* Signature Bioscience, Inc., San Francisco, CA 94107.

[4]*Present address:* Department of Biochemistry, University of Wisconsin, Madison, WI 53706.

[5]*Present address:* Department of Molecular and Cell Biology, University of California, Berkeley, CA 94720.

[6]*Corresponding author:* Department of Genetics, Life Sciences Bldg. C418, 1057 Green St., University of Georgia, Athens, GA 30602-7223. E-mail: bender@arches.uga.edu

end with a small C-terminal extension that is not highly conserved within the family.

Cleavage of precursor molecules by the convertases occurs after basic residues, most often Lys-Arg (K-R↓) or Arg-Arg (R-R↓) sequences (Rockwell *et al.* 1997). PC2 is able to cleave after Lys-Lys (K-K↓) sequences, a property potentially due to its unique oxyanion hole residue (Shennan *et al.* 1991). Because of its more diverse array of cleavage sites, PC2 is often described as the most highly adapted member of the subtilisin-like proprotein convertase family (Rouille *et al.* 1995a). PC2 displays a neuroendocrine tissue-specific expression pattern (Smeekens *et al.* 1991) and is responsible for the activation of peptide hormones including proinsulin, proglucagon, and proopiomelanocortin in mice (Benjannet *et al.* 1991; Rouille *et al.* 1994; Furuta *et al.* 1998). Loss of PC2 activity has been linked to diabetes, obesity, and breast cancer (Yoshida *et al.* 1995; Steiner *et al.* 1996; Brar and Lowry 1999).

The gene encoding the Drosophila homolog of mammalian PC2 has been identified and named *amontillado* (*amon*; Siekhaus and Fuller 1999). The *amon* protein is 75% identical to human PC2 in the catalytic domain and 66% identical overall. Whole-animal Northern blots show that *amon* expression peaks during late embryogenesis and in the adult. *amon* is expressed in a subset of cells of the brain and ventral nervous system during late embryogenesis and in a smaller set of brain and ventral nervous system cells during first and second instar larval development (Siekhaus and Fuller 1999). Recently, the *amon* protein has been shown to be an active protease on a KR containing synthetic peptide when expressed in Drosophila S2 cells with the d7B2 protein, a homolog of the 7B2 helper protein that functions in maturation of PC2 (Hwang *et al.* 2000). Initial investigation of *amon* function indicated a requirement for *amon* during hatching behavior (Siekhaus and Fuller 1999). However, this study lacked *amon*-specific mutants, instead using overlapping deficiencies that remove the chromosomal region including *amon* and flanking genes.

To identify point mutations that inactivate *amon*, we have screened for EMS-induced mutants that are lethal when heterozygous to chromosomal deficiencies that remove *amon*. DNA sequencing shows that one of the two complementation groups identified corresponds to *amon*. Six *amon* missense mutations have been identified while three *amon* mutations are predicted to result in truncation of the *amon* protein. *amon* mutants display partial embryonic lethality and fail to complete the first to second instar larval molt. *amon* mutants can be rescued by heat-shock-induced expression of the *amon* protein and some rescued animals arrest at the second to third instar larval molt. These data indicate that *amon* is required during embryogenesis and larval development and support the hypothesis that AMON acts to proteolytically process peptide hormones that regulate hatching, larval growth, and larval molting.

MATERIALS AND METHODS

Fly strains: The *red e* and *red* parental strains, *Df(3R)Tl-X/TM3*, *Df(3R)ro80b/TM3*, and w^{1118}; *Ly/TM6B*, *P{w[+mW.hs]=Ubi-GFP.S65Y} PAD2*, *Tb* (referred to here as *TM6B GFP Tb*), were obtained from the Bloomington Stock Center.

EMS mutagenesis and F_2 lethal screens: Males homozygous for a marked third chromosome (*red e* or *red*) were treated with 0.025 m EMS using the procedure of Lewis and Bacher (1968). Mutagenized males were mated *en masse* to *TM3 Sb/TM6B* virgin females at 25°. Individual F_1 progeny (*red e* or *red/TM6B* and *red e* or *red/TM3 Sb*) were then pair-mated to *Df(3R)ro80b/TM3 Sb*, *Df(3R)Tl-X/TM3 Ser*, or *Df(3R)Tl-X/TM3 Sb* flies and crosses were scored for absence of the F_2 progeny class that was heterozygous for the mutagenized chromosome and the deficiency. If this class was absent, stocks were established from *red e* or *red/TM3* siblings and then tested for the ability to complement *Df(3R)Tl-X* or *Df(3R)ro80b*.

We recovered 16 lethal mutations and 1 visible mutation that fail to complement either *Df(3R)Tl-X* or *Df(3R)ro80b* from 5300 fertile pair matings scored. Nine lethal mutations and the visible mutation fail to complement both *Df(3R)Tl-X* and *Df(3R)ro80b* and are described in this manuscript. Each of these mutations was placed in complementation groups by complementation tests to all other mutations within the *amon* interval defined by the overlap between *Df(3R)Tl-X* and *Df(3R)ro80b*. The remaining 7 lethal mutations that fail to complement only one of these deletions and thus map outside of the *amon* interval have been described elsewhere (Kidd *et al.* 1999). Of the EMS-induced mutations described here, $amon^{C254Y}$ was induced on a *red* background chromosome, $amon^{G473R}$, $amon^{Q507sa}$, and doc^{99} were induced on an *ebony* background, and the remainder of the mutations was induced on a *red e* background. Allelism of the *l(3)rK344 P*-element insertion mutation to *Toll* was established by complementation tests to the $Toll^{r3}$ allele carried out at the restrictive temperature (Lindsley and Zimm 1992).

DNA sequence analysis: Primers for PCR amplification were designed using the Oligo 4.0 program (Molecular Biology Insights) and were synthesized by the Molecular Genetics Instrumentation Facility (MGIF) at the University of Georgia using an ABI 394 synthesizer. Ten pairs of PCR primers (18–20 mers) were used for PCR amplification of *amon* protein-coding sequences and DNA sequencing. PCR product sizes range from 387 to 840 bp. Primer sequences are available upon request. Initial attempts to PCR amplify DNA from genomic DNA extracted from homozygous mutant larvae were unsuccessful. We therefore sequenced PCR products amplified from genomic DNA of flies heterozygous for lethal mutations and a balancer chromosome. Mutations were identified by comparison of sequence from mutant heterozygotes to that obtained from the homozygous parental strain upon which the mutations were induced. Genomic DNA was obtained for each mutant line using a small-scale phenol/chloroform extraction (10–50 flies).

DNA was amplified using EnzyOne polymerase (ENZYPOL). The DNA template (1 μl) to be amplified was added to a solution of 1.5 mm $MgCl_2$, 2.5 μl 10× NH_4 reaction buffer, 200 μm dNTP, 2.0 μl each of the sense and antisense primers diluted to 5 pmol/μl, 0.25 μl EnzyOne 500 unit DNA polymerase, and dH_2O to bring the final volume to 25 μl. Products were analyzed on a 1.0% agarose gel and were purified with a High Pure PCR product purification kit (Boehringer Mannheim, Indianapolis).

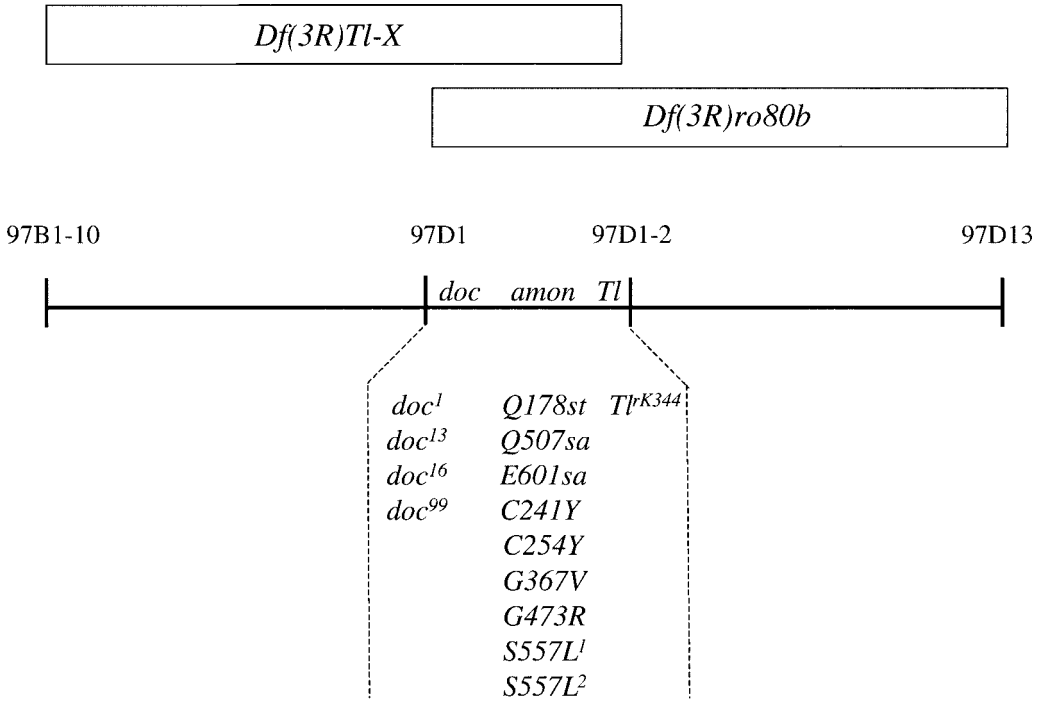

FIGURE 1.—At least three complementation groups map within the *amon* chromosomal interval. The extent of two deficiencies that remove *amon*, *Df(3R)Tl-X* and *Df(3R)ro80b*, is indicated by the open bars at the top, and cytological endpoints of these deficiencies are shown at the center. Two complementation groups identified in this screen (*doc* and *amon*) and the *Toll* gene map to the overlap between these two deficiencies. Mutant alleles within each complementation group are listed at the bottom. For *amon* mutant nomenclature, the first affected amino acid is followed by the mutant change (sa, splice acceptor; st, stop).

Double-stranded sequencing of a minimum of two independent PCR products was conducted by MGIF using an ABI 373 automated sequencer. Sequence data were analyzed with the Sequencher 3.0 program (Gene Codes Ann Arbor, MI). During the course of our sequence analysis we noted a minor error in the amino acid sequence reported by SIEKHAUS and FULLER (1999). Amino acids 344–348 are incorrectly reported as glutamate, aspartate, aspartate, cysteine, and asparagine (E D D C N). The correct order should be aspartate, aspartate, cysteine, asparagine, cysteine (D D C N C). We also identified 19 polymorphisms within *amon* coding sequences. These polymorphisms are reported elsewhere (RAYBURN *et al.* 2002).

Lethal phase determination: Twenty-five *yw;amon/TM6B GFP Tb* males were mated to 25 *yw; Df(3R)Tl-X/TM6B GFP Tb* virgin females in an egg collection apparatus at 25°. As a control, 25 *red e/TM6B GFP Tb* males were mated to 25 *Df(3R)Tl-X/TM6B GFP Tb* virgin females. Flies were fed yeast paste and grape juice agar egglay plates were changed daily. On the third day a 10-hr egg collection was taken and 200 eggs from this collection were kept for further analysis. F_1 larvae were scored at 36, 60, 96, and 120 hr after egg laying (ael) corresponding to the approximate midpoints of the first larval instar, second larval instar, and third larval instar and to pupariation. Mutant larvae were transferred to fresh egglay plates after each scoring. F_1 larvae were scored for the dominant green fluorescent protein (GFP) marker to separate *amon* (or *red e* parental) */Df(3R)Tl-X* flies lacking GFP from siblings carrying the *TM6B GFP Tb* balancer chromosome. The percentage of survival of *amon* mutant or parental larvae was calculated by dividing the number of mutant or parental animals alive at each time point by the Mendelian expectation for mutant or parental hemizygotes from these crosses (25%). To examine terminal phenotypes, *amon* mutants found dead at 36, 60, and 96 hr ael and live wild-type sibling larvae collected at the same times were placed in a polyvinyl lactophenol mounting medium on glass slides. Photographs were taken with a Zeiss Axiophot microscope.

Rescue: A previous study (SIEKHAUS and FULLER 1999) described the construction of the *hs-amon* transgene and showed that *amon* mRNA is induced following heat shock. In our experiments 30 *yw; +/+; amon/TM3 Sb Ser* y^+ *e* males were mated to 30 *yw; hs-amon/hs-amon; Df(3R)Tl-X e/TM3 Sb Ser* y^+ *e* virgin females in an egg collection apparatus at 25°. In parallel, 30 *yw; +/+; amon/TM3 Sb Ser* y^+ *e* males were mated to 30 *yw/yw; +/+; Df(3R)Tl-X e/TM3 Sb Ser* y^+ *e* females. Ten-hour egg collections (n = 200 eggs) were taken as described above. Animals were heat-shocked (30 min at 37°) every 12 hr beginning at 36 hr ael. Plates were scored at 36, 60, 96, and 120 hr ael and at subsequent times until adulthood. Mutant animals [*yw; amon/Df(3R)Tl-X*] were recognized by the *yellow* marker. Percentage of survival was calculated by dividing the number of mutant animals alive at each time point by one-half the total number of wild-type non-*yellow* siblings present at 36 hr. In the course of these experiments, we found that percentage of survival of $amon^{C241Y}$*/Df(3R)Tl-X* mutants is reproducibly lower in the *TM3 Sb Ser* y^+ *e* background than in the *TM6B GFP Tb* background (data not shown). This fact, plus the observation that heat-shock treatment (in the absence of *hs-amon* transgenes) reduced the viability of *amon* mutants, accounts for differences in viability of $amon^{C241Y}$*/Df(3R)Tl-X* mutants in Figure 6A and Table 3.

RESULTS

Isolation of candidate *amon* mutations: The *amon* gene has been mapped to the 97D1 region of chromosome 3R by *in situ* hybridization to the overlapping deficiency chromosomes *Df(3R)ro80b* and *Df(3R)Tl-X* (SIEKHAUS and FULLER 1999). To generate point mutations in *amon*, we screened for EMS-induced lethal and visible mutations in this interval. From a total of 5300 mutagenized chromosomes, we identified nine lethal mutations and one visible mutation that fail to complement both *Df(3R)ro80b* and *Df(3R)Tl-X* and are therefore candidate *amon* mutations (see MATERIALS AND METHODS). Figure 1 shows that these mutations, plus three

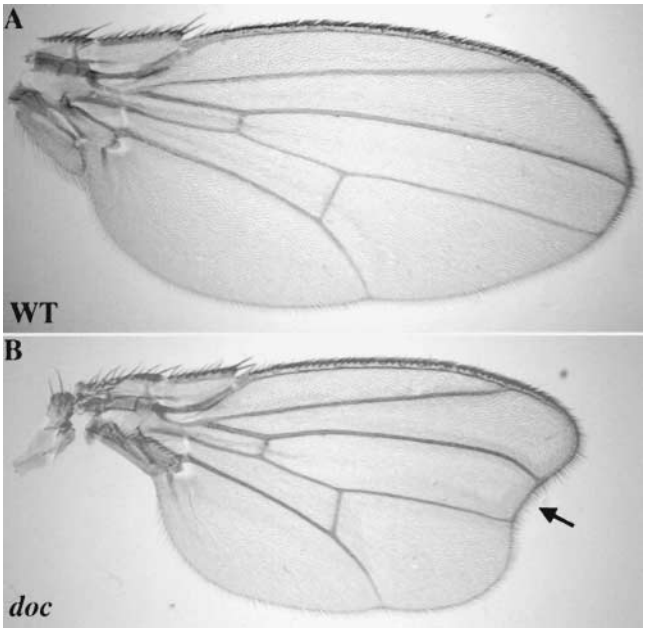

FIGURE 2.—The *docked*[1] mutant displays a visible wing phenotype. (A) A wild-type (*CS*) wing; (B) the irregularly shaped wing of a *doc*[1] (*doc*[1]/*Df(3R)Tl-X*) mutant. The wing margin of the *doc*[1] mutant appears normal, but distal portions of the wing are absent, resulting in a docked-wing appearance (arrow).

other lethal EMS-induced mutations and a lethal *P*-element insertion mutation [*l(3)rK344*], kindly provided by K. Anderson, fall into three complementation groups. We show below that the largest of these, containing nine lethal mutations, corresponds to *amon*.

Of the remaining two complementation groups, one corresponds to the *Toll* gene and is represented by the *Toll*[rK344] allele (Figure 1). The final group identified consists of three lethal mutations and one recessive visible mutation, *docked*[1] (*doc*[1]). When heterozygous to *Df(3R)Tl-X* or *Df(3R)ro80b*, *doc*[1] mutants exhibit irregularly shaped wings with reduced size relative to wild type (Figure 2). *doc*[1] mutants have normal wing margins but appear to lack distal wing derivatives, resulting in a docked wing appearance. The three lethal mutations in the *docked* complementation group are viable when heterozygous to *doc*[1] but partially or completely fail to complement the docked wing phenotype, with *doc*[99] being the strongest and *doc*[13] the weakest allele in this regard. When hemizygous to *Df(3R)Tl-X*, *doc* mutants die during embryogenesis and during the first larval instar (data not shown).

***amon* gene structure:** To facilitate identification of *amon* mutants by DNA sequencing, we first determined the *amon* gene structure by comparing a previously published *amon* cDNA sequence (SIEKHAUS and FULLER 1999) to the Drosophila genome sequence (ADAMS *et al.* 2000). Table 1 shows the predicted *amon* splice donor and acceptor sequences and exon and intron sizes while Figure 3 shows the position of exon/intron boundaries relative to *amon* cDNA sequences. The *amon* gene is composed of 12 exons and spans ~16 kb of genomic sequence. The first of the gene's 11 introns is 9687 bp in length, while the remaining introns are all <1000 bp (range, 54–842 bp). While determining the gene structure of *amon*, we discovered that the first 43 nucleotides of the published cDNA (SIEKHAUS and FULLER 1999) do not align with upstream *amon* genomic DNA. Because these nucleotides match sequences within more 3′ areas of the cDNA (see RAYBURN *et al.* 2002) and

TABLE 1

Exon-intron junctions of the *amon* gene

		Sequence at exon-intron junctions			
Exon no.	Exon size (bp)	5′-splice donor		3′-splice acceptor	Intron size (bp)
1	>545	GGC CCG gtaagt	. . .	ttacag CTG GTC	9687
2	108	CCG GCG gtgagt	. . .	ccgcag GTG CAT	842
3	271	GAT G gtgagt	. . .	gcccag GC GTG	90
4	38	AAT TAT gtgagt	. . .	ttccag AAC GCC	449
5	77	AAC AG gtaagt	. . .	tttcag C CAT	343
6	89	GCA G gtaagt	. . .	caacag GC ATT	527
7	176	AAT GAG gtacgg	. . .	ccgcag GGT CGA	71
8	314	GCC AA gtgagt	. . .	tggcag T CCT	245
9	234	CCA CA gtgagt	. . .	acgcag G GCC	68
10	166	ACC AA gtaagt	. . .	ccatag A TCG	89
11	117	TTG GAG gtagta	. . .	ccacag GCT CGC	54
12	1719				

Exon-intron boundary sequence is given for each junction in the *amon* gene. Exon sequence is in uppercase letters and intron sequence is in lowercase. The exon number and size refer to the exon that precedes the given boundary, while the intron size refers to the intron contained by the given boundary. Exon and intron sizes and junction sequences were elucidated by comparing the known *amon* cDNA sequence to the published Drosophila genomic sequence (SIEKHAUS and FULLER 1999).

```
     ATAATGGCGTCCGTCGGTACCGCTGGCGAACAGTACTCAGCGCGCAGCGCCCCAGTGAAGTTCGTGGCAGCGCACAAAGACTCCAGACGAAGTACATAGA  100
     AACAGAATTTCAGGCGGAAGGAAAGCACAACAAGCTCCATAGAAGGGGCCAAAAATACACAATAAAGAAAACAAATTGCAACCACAACAAGAGGATATTT  200
     TGCCAACCGAGCAACTTGATCCTGGCTACCCAATTCGCGTCGCCAATTCGCAGAGTGTGCAGTGGAGCGCGTCCTTTATTTTCGTCAGCACTTCGGTATC  300
     CTGCCAACGGAAAAAATCACCCAAAGGACGCCCCACGCACCAACTGTTTGTACGGGCTGCCAGAGTTGCCCCATCGCCGCCAGGAGTTCAGAGGCCAGGA  400
     GGAACCCGCAGGACCAAGGCGTCCAATCTGAATTCCATGGCAGCAGCCACATGGAGCTGGCTGTTGGCCCCATTCCTGCTCCTCCACTGGGCCAGTGCAG  500
                                        M  A  A  A  T  W  S  W  L  L  A  P  F  L  L  L  H  W  A  S  A
     GAGCGGGCGGAGGAGCAGGCGGCTCGGGAGCGGGACTGAGCGGCCCCGCCGTCTTTACCAGCTCCTTCCTGGTGCGCTTCCGGCGCGGAGTGGACAACTC  600
  22 G  A  G  G  G  A  G  G  S  G  A  G  L  S  G  P  A  V  F  T  S  S  F  L  V  R  F  R  R  G  V  D  N  S
     GTTTGCCCATGATGTGGCCGACAAGTACGGCTTCGACAACCTAGGCCCGCTGGTCGGCGCCGATGGACACGAGTATCACTTCAAGCACCGGACCCTTCCA  700
  55   F  A  H  D  V  A  D  K  Y  G  F  D  N  L  G  P  L  V  G  A  D  G  H  E  Y  H  F  K  H  R  T  L  P
     CATGCCCGCTCCAGGAGGAGTCTGACGCACACACGGGCCCTCAAGAGCCATCCGGCGGTGCATACGGCCGTGCAACAGCCGGGATTCAAGCGGGTTAAAC  800
  89  H  A  R  S  R  R  S  L  T  H  T  R  A  L  K  S  H  P  A  V  H  T  A  V  Q  Q  P  G  F  K  R  V  K
     GTGGCCTGCGGCCGGCGGTGCCCGCCATTCACGGCATGAAGTTCGACCTGAAAGTTGGCGAGGGCAATCGGATTGACGAGGAGCCCACTGACCCCTACTT  900
 122 R  G  L  R  P  A  V  P  A  I  H  G  M  K  F  D  L  K  V  G  E  G  N  R  I  D  E  E  P  T  D  P  Y  F
     TCCCATGCAATGGTACCTCAAGAACACGGGTCAGAATGGCGGCAAAGTCAGACTGGATCTGAATGTGCAGGCTGCCTGGGCCCAGGGAATCACCGGGAAG  1000
 156   P  M  Q  W  Y  L  K  N  T  G  Q  N  G  G  K  V  R  L  D  L  N  V  Q  A  A  W  A  Q  G  I  T  G  K
     AATGTTACGACGGCCATCATGGATGATGGCGTGGACTACATGCATCCGGATCTGAAATTCAATTATAACGCCGAGGCCAGTTATGACTTCAGCAGTAACG  1100
 189  N  V  T  T  A  I  M  D  D  G  V  D  Y  M  H  P  D  L  K  F  N  Y  N  A  E  A  S  Y  D  F  S  S  N
     ATCCCTTTCCGTATCCCCGATACACCGACGACTGGTTCAACAGCCATGGAACTCGTTGTGCCGGCGAAGTGGCTGCTGCCAGAGATAATGGAATTTGCGG  1200
 222 D  P  F  P  Y  P  R  Y  T  D  D  W  F  N  S  H  G  T  R  C  A  G  E  V  A  A  A  R  D  N  G  I  C  G
     CGTTGGCGTTGCTTATGACAGCAAAATCGCAGGCATTCGCATGCTGGATCAGCCGTACATGACGGACCTAATCGAGGCCAACTCCATGGGCCACGAGCCG  1300
 256   V  G  V  A  Y  D  S  K  I  A  G  I  R  M  L  D  Q  P  Y  M  T  D  L  I  E  A  N  S  M  G  H  E  P
     CACAAAATCCACATATACAGCGCCTCCTGGGGTCCCACCGATGATGGCAAGACCGTGGACGGTCCCCGGAATGCCACCATGCGAGCGATAGTCCAGGGCG  1400
 289  H  K  I  H  I  Y  S  A  S  W  G  P  T  D  D  G  K  T  V  D  G  P  R  N  A  T  M  R  A  I  V  Q  G
     TCAATGAGGGTCGAAATGGCCTGGGCAACATATATGTTTGGGCATCCGGCGACGGGGGCGAGGAGGATGACTGCAACTGTGACGGCTATGCCGCCTCCAT  1500
 322 V  N  E  G  R  N  G  L  G  N  I  Y  V  W  A  S  G  D  G  G  E  E  D  D  C  N  C  D  G  Y  A  A  S  M
     GTGGACCATTTCCATTAACAGTGCCATTAACGACGGCCAGAACGCCCACTACGACGAGAGCTGCAGCTCCACGCTGGCGTCCACATTCAGCAACGGAGCC  1600
 356   W  T  I  S  I  N  S  A  I  N  D  G  Q  N  A  H  Y  D  E  S  C  S  S  T  L  A  S  T  F  S  N  G  A
     AAGGACCCCAACACGGGCGTTGCCACCACGGACCTCTATGGCAAGTGCACGACCACCCACTCGGGCACCAGTGCGGCGGCGCCCGAAGCAGCGGGCGTCT  1700
 389  K  D  P  N  T  G  V  A  T  T  D  L  Y  G  K  C  T  T  T  H  S  G  T  S  A  A  A  P  E  A  A  G  V
     TTGCCCTGGCCTTGGAGGCCAATCCTCAGCTGACTTGGCGGGACATACAGCATCTGACGGTGCTGACATCGAAGCGCAACTCGCTGTTCGATGCCAAGAA  1800
 422 F  A  L  A  L  E  A  N  P  Q  L  T  W  R  D  I  Q  H  L  T  V  L  T  S  K  R  N  S  L  F  D  A  K  N
     CCGATTCCACTGGACAATGAACGGCGTGGGCCTGGAGTTCAACCACCTATTCGGGTTCGGAGTGCTGGACGCCGGCGCCATGGTCACACTATCCAAGCAG  1900
 456   R  F  H  W  T  M  N  G  V  G  L  E  F  N  H  L  F  G  F  G  V  L  D  A  G  A  M  V  T  L  S  K  Q
     TGGCATTCAGTGCCACCGCGCTATCATTGCGAGGCGGGCGAGCTTACCCAGCCACAGGCCATTGTTATGGGTCGTTCGCTCTTCTGGGAGATCAAAACCG  2000
 489  W  H  S  V  P  P  R  Y  H  C  E  A  G  E  L  T  Q  P  Q  A  I  V  M  G  R  S  L  F  W  E  I  K  T
     ATGCTTGCAAGGGCACCGACACGGAGGTCAACTATTTAGAACACGTGCAGGCGGTGATCTCGGCAAATGCCTCACGACGCGGGGATCTTGAACTTTTCCT  2100
 522 D  A  C  K  G  T  D  T  E  V  N  Y  L  E  H  V  Q  A  V  I  S  A  N  A  S  R  R  G  D  L  E  L  F  L
     TACATCGCCAATGGGCACACAATCCATGATCCTGTCGAGGCGCGCCAACGATGATGACCACCGCGATGGCTTCACCAAATGGCCCTTTATGACCACTCAC  2200
 556   T  S  P  M  G  T  Q  S  M  I  L  S  R  R  A  N  D  D  D  H  R  D  G  F  T  K  W  P  F  M  T  T  H
     TCGTGGGGCGAGTATCCGCAGGGGACCTGGAAATTGGAGGCTCGCTTCAACTCGCCCCAAACACGACACGGCAATCTGCTGGAATGGTCCTTGGTCCTGC  2300
 589  S  W  G  E  Y  P  Q  G  T  W  K  L  E  A  R  F  N  S  P  Q  T  R  H  G  N  L  L  E  W  S  L  V  L
     ATGGCACCAAGGAGGCGCCCTATCGCACCCTGCACCCCTCGTCGCCGCACTCCAAGCTGGCCATTGTGAAGAAGGCGCACGAGGACAAGAAGATGAAGTA  2400
 622 H  G  T  K  E  A  P  Y  R  T  L  H  P  S  S  P  H  S  K  L  A  I  V  K  K  A  H  E  D  K  K  M  K  *
     GGGCGGGTCGCGCAGAGGGTCAGAGGTCAGGTCCAGATAAACATCCGCGTAGCGACGTCCATTAGGCAGCTTGGCGTTTTATCAACGAGTTTAGTGTGAG  2500
     GTTCAATAAAAGTGCTGGCTGTGTTTTATTTTGGAATAGGATTGATTGAGATTAAACATTTTATTTCGATTGTGTTTGTCCTTTGTGTAACTTCTAATAT  2600
     TTGTCATTTGCGTTGGATCTGTAGAACTGAAAGTTCATTTAAGCGAGGGATGTCCTTTATCATTTCCGTTTTTGTAATTAGTTTTCTGATTTGGTGAGCT  2700
     AAGCGCCCAGGGTGCCACAAAATCACTTCATTCGCCGTTTAAACTTATTCTGGAAAGCGCACATTTGCCACAGTATAACAGATTTATCAAAATTCTGCAC  2800
     TCAACACCATAATCCGTTGAGTGTCCTAGCGAACTCTGTAGTCGATATCGAAGGCAACCACAAAATAAGAACATAGAAAACAGGTATAGCAGGTATATTT  2900
     GAATGCGTAGCAAGACTAGGAGGCGGGGAATAGAGATATATAATAAAACTAGAACAAAGAAAACAGGATAAACCCTATGTAAATGTGTAATATCTATATG  3000
     TATGCATACCCTATCTTTAACTGCGTCCTATGCTGTAGCTTATAACTCTTTCTAGTATAAAATACAAACTAAACAAAGTATTTACACACGTATTTTAAAG  3100
     CTTTGTCCTTTGTTTTCCATCCTATATATACACGAATATACCTACATACATGCATATACATATGTACTTAAAGGATACTTAGCAAAAACATAAAATGTTA  3200
     ATCCCATTATTGCGGAACATGTTTGTCGCTTAACTTTGGTTGCAAGCCAAAATCTGCTTTAATTTGGATACAACTCGTACGTGTAAAATGCATTTACATA  3300
     CATAGTTTTCCTTTCAGTTTCTTTCGGGGGCCAAAAAAACCACAACATAGTAACATTAATTGTGTGAAACCAGATTCACGATTGTGTCGTAAAACGGAGC  3400
     GTGTGTTTTGAAAATACATAAACAAATGTTAAAGTACAAGTGCATAAACCTTAACGGTGAGCAGAGAGATACAGATACGGATTGTTTTACCTAGTCTAAT  3500
     AACTGAGATACAGCGCATTGTTAAAGTTTACCGATAATGTGCGAGAGGAATAAAATATATATATATACACAGAACCATATATGAAGTACATACACGTG  3600
     TAATTATTAATCAAAAACCACATGAAGAGGTGACGGCGGAAACTGTGGMATAACCATTATATACATACACCGAATATTNAACTATATATATGCATAAATK  3700
     NATGATACGTATATATAAACCACAAAATAAACGCAAGGAGTATCTTATGTGGCCGTTAAGTTGATTTTTGATGTTGTAGATACAAGAAGTAGCACCAATA  3800
     GATGCACCATACCACTCAAAATTATAGAAAGATGTGAGAATGCTAATGCAAAACCGATATTTGATTGCAAATTTAATTATTTCCTATAGCACAAAATTTG  3900
     TTTTTGTCTTTTGGTGCGGTTTTGTCATTTCCATGTAATTGAACAGAAAGAGAATTTAATTTTGTAAATAAAAGTTAAGAAAAAACGCAAAAAAAAAAAA  4000
     AAAAAAAAAAAA
```

FIGURE 3.—A composite *amon* cDNA sequence. The first 64 nucleotides of this sequence derive from the BDGP *amon* EST with the greatest 5′ extent (clone no. RE06156). The remainder of the cDNA sequence is composed of nucleotides 44–3392 of a previously published *amon* cDNA (SIEKHAUS and FULLER 1999). The vertical bars within the *amon* cDNA sequence refer to intron/exon boundaries as deduced by comparison with the genomic sequence. The residues comprising the catalytic triad are circled. The oxyanion hole aspartate residue is boxed.

because 11 *amon* expressed sequence tags (ESTs) sequenced by the Berkeley *Drosophila* Genome Project (BDGP) contain sequences 5′ of the start of the published cDNA that do match genomic sequences, we believe that the reported *amon* cDNA contained a cloning artifact at the 5′ end. The cDNA sequence shown in Figure 3 is a composite of the BDGP cDNA with the greatest 5′ extent (clone no. RE06156) and the pre-

TABLE 2

Mutations in the *amon* gene

Mutant	Mutation	cDNA bp	Predicted effect
Q178st	CAG → **T**AG	968	Gln 178 → Stop
Q507sa	ag → aa (intron)	NA	Incorrect splicing
E601sa	ag → aa (intron)	NA	Incorrect splicing
C241Y	TGT → T**A**T	1158	Cys 241 → Tyr
C245Y	TGC → T**A**C	1197	Cys 254 → Tyr
G367V	GGC → G**T**C	1536	Gly 367 → Val
G473R	GGG → **A**GG	1853	Gly 473 → Arg
S557L[1]	TCG → T**T**G	2106	Ser 557 → Leu
S557L[2]	TCG → T**T**G	2106	Ser 557 → Leu

NA, not applicable.

viously published *amon* cDNA (Siekhaus and Fuller 1999).

Identification of *amon* mutants: To determine which complementation group in the *amon* interval corresponds to the *amon* gene, we sequenced PCR products amplified from genomic DNA of flies heterozygous for lethal mutations and a balancer chromosome. The sequence generated was compared to the genomic DNA sequence from the parental chromosome and to genomic sequence from sibling chromosomes heterozygous to the same balancer chromosome to identify base pair changes induced by EMS. Initial sequencing of *amon* genomic DNA encoding exons 9–12 from lethal mutants in both complementation groups showed that four members of the larger complementation group contained mutations in *amon* while none of the members of the smaller complementation group contained such mutations, identifying the larger group as the *amon* complementation group (see Figure 1). Subsequent sequencing efforts focused on this complementation group.

Table 2 shows the mutation and predicted effect on coding sequences for each of the nine *amon* complementation group members and Figure 4 shows the location of each mutation relative to *amon* coding sequences. Three mutations are predicted to lead to truncation of the *amon* protein. One, $amon^{Q178st}$, results in a stop codon and is predicted to produce a protein lacking most of the catalytic domain and all of the P domain of the protein. Two others, $amon^{Q507sa}$ and $amon^{E601sa}$, affect conserved splice acceptor site dinucleotides. The *Q507sa* mutation is predicted to disrupt the joining of exon 9 to exon 10, resulting in a truncated protein. This mutant protein is predicted to lack the final 147 amino acids if there is readthrough into intron 9 to an immediate stop codon (see Table 1) or predicted to lack amino acids 508–562 if the subsequent splice acceptor site preceding exon 11 is used, thereby skipping exon 10. Either of these possibilities would result in a protein lacking most of the P domain. The *E601sa* mutation is predicted to disrupt the correct joining of exon 11 to exon 12, thus causing 7 extraneous amino acids to be added to the protein before a premature stop codon occurs if there is readthrough into intron 11. This mutation would thereby eliminate 23 amino acids of the P domain and all 30 amino acids of the C-terminal extension.

Of the six *amon* missense mutations, four map to the catalytic domain (Figure 4) and each of these four affects highly conserved residues in the kexin subfamily of subtilisin-like serine proteases or "subtilases" (Siezen and Leunissen 1997). The first of these, $amon^{C241Y}$, is predicted to result in a substitution of cysteine 241 by a tyrosine residue. This cysteine is conserved in 30 of 31 kexin subfamily members (Siezen and Leunissen 1997). Homology modeling of the catalytic domain of subtilases has been carried out on the basis of the crystal structure of seven subtilases (Siezen and Leunissen 1997). The $amon^{C241Y}$ missense change is predicted to map within helix C of this structure, a short α-helix in the core of the protein directly under the catalytic site of the enzyme (see Figure 1 of Siezen and Leunissen 1997). The cysteine residue is predicted to be a partner in a disulfide bond among members of the kexin subfamily (Siezen and Leunissen 1997).

The $amon^{C254Y}$ mutation is also predicted to change a cysteine residue conserved in the kexin subfamily (29 of 31; Siezen and Leunissen 1997) to a tyrosine. Within the subtilase catalytic domain model, the $amon^{C254Y}$ missense change is predicted to map within a variable loop at the surface connecting helix C to a conserved β-sheet strand (e3). This cysteine is predicted to be a partner in a separate disulfide bond in kexin subfamily members (Siezen and Leunissen 1997).

The $amon^{G367V}$ mutation is predicted to result in substitution of glycine 367 by valine. This conserved glycine residue (27 of 31) maps to a conserved loop between two β-sheet strands (e6 and e7; Siezen and Leunissen 1997, Figure 1). Finally, the $amon^{G473R}$ missense change (arginine for glycine 473) maps to a conserved loop between helix G and helix H near the C terminus of the catalytic domain. This glycine residue is completely conserved (31 of 31) among the kexin subfamily and strongly conserved (92 of 126) among the entire subtilase protein family (Siezen and Leunissen 1997).

The remaining two missense mutations, $amon^{S557L1}$ and $amon^{S557L2}$, affect the same nucleotide and are predicted to result in substitution of serine 557 by a leucine residue within the P domain. Although no P-domain structures have yet been determined, a model of P-domain structure has been proposed on the basis of analysis of P-domain sequences from seven human kexin protein family members plus Kex2p (Lipkind *et al.* 1998). The $amon^{S557L}$ missense change maps within a conserved loop between two β-strands (β_4 and β_5) of the proposed β-barrel-like structure.

***amon* mutants exhibit embryonic lethality, delays in larval growth, and defects in larval molting:** Table 3 shows the percentage of *amon* mutants surviving to a given time after egg laying when heterozygous to the

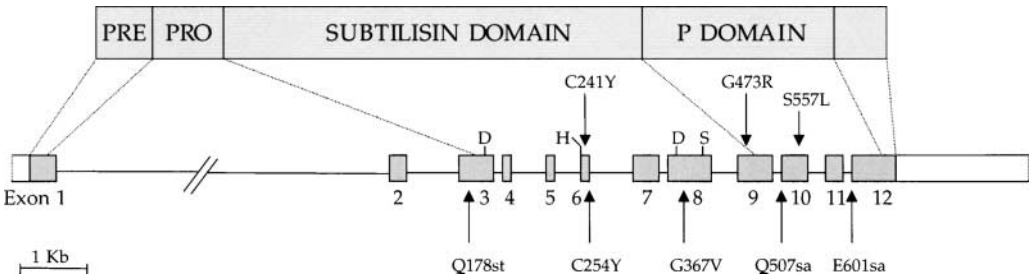

FIGURE 4.—Mutations within the *amon* gene. The location of each mutation within the gene structure of *amon* is indicated by an arrow. The domain structure of AMON is shown at the top (SIEKHAUS and FULLER 1999). Boxes and lines below indicate exons and introns, respectively. Shaded boxes indicate *amon* protein-coding sequence. The catalytic triad (D, H, S) and the oxyanion hole residue (D) in exon 8 are indicated.

Df(3R)Tl-X chromosome. Animals were scored at 36, 60, 96, and 120 hr ael, times corresponding in wild-type animals to the approximate midpoints of the first, second, and third larval instars and to pupariation, respectively. All *amon* mutants demonstrate some degree of embryonic lethality, with a range of 37% ($amon^{E601sa}$) to 84% ($amon^{C254Y}$) of expected larvae surviving at 36 hr ael (Table 3). Very few *amon* mutants survive at 96 hr ael (range, 0–8% of expected), indicating that most *amon* mutants that complete embryogenesis and hatch from the egg die during larval development. Although the 60- and 96-hr time points correspond to the midpoints of second and third larval instar development in wild-type animals, *amon* mutants surviving at this time were dramatically smaller than wild-type sibling controls. Surviving larvae were also lethargic and unresponsive to an external stimulus and the few animals surviving to 96 and 120 hr ael failed to exhibit larval wandering behavior (data not shown). No *amon* mutant larvae pupariated and none survived to adulthood (Table 3).

amon mutants that arrest during larval development are defective in larval molting. The majority of arrested mutant larvae show the presence of duplicated pairs of larval mouth hooks (Figure 5) identifiable by morphology as first and second instar larval mouth hooks. Thus *amon* mutants that complete embryogenesis and hatching exhibit delayed growth during larval development and arrest during the first to second instar larval molt.

***amon* mutants can be rescued by heat-shock-driven expression of AMON:** Expression of AMON from a heat-shock-inducible transgene (*hs-amon*; SIEKHAUS and FULLER 1999) partially rescues the embryonic lethality of the *amon* mutants (71% survival *vs.* 43% for no transgene controls when scored at 36 hr ael). Figure 6A shows that expression of AMON from the transgene also increases the survival of *amon* mutants at 60 and 96 hr ael relative to no transgene controls. In contrast to controls lacking the *hs-amon* transgene, rescued *amon* mutants [*yw; hs-amon;* $amon^{C241Y}$*/Df(3R)Tl-X*] were comparable in size to wild-type second and third instar siblings (data not shown). As shown in Figure 6A, expression of AMON is not sufficient to rescue 100% of *amon* mutants to later time points. Examination of *amon* mutants carrying the *hs-amon* transgene that arrest between the 60- and 96-hr time points showed that these animals arrest with duplicated mouthparts consisting of one pair of second and one pair of third instar larval mouth hooks (Figure 6B). Thus expression of AMON allows these mutants to complete the first to second instar larval molt and to progress through second instar larval development before arresting during the second to third instar larval molt.

In this experiment, rescue of the *amon* mutants continued to the adult stage, with one $amon^{C241Y}$*/Df(3R) Tl-X* mutant rescued to adulthood. Although the total development time from egg to adulthood was ~25% greater than normal, the resulting female was fertile. Nine subsequent rescue experiments using a 30-min heat-shock pulse delivered every 12 hr or every 24 hr also produced adult *amon* mutant flies, recognizable by the absence of balancer chromosome markers, in the range of 2–43% of expected. In these experiments, control *amon* mutants lacking the *hs-amon* gene never survived beyond 96 hr ael.

DISCUSSION

Isolation of *amon* point mutants: We have identified point mutations that inactivate *amon*, the Drosophila homolog of the vertebrate prohormone convertase PC2, by screening for EMS-induced lethal and visible mutants that fail to complement overlapping deficiencies that remove the *amon* gene. Two complementation groups were identified in our screens (Figure 1). DNA sequencing showed that each of the nine members of the larger complementation group exhibits a DNA sequence change in *amon* gene sequences that is predicted to result in an altered *amon* protein (Table 2; Figure 4). This result and the fact that heat-shock-induced expression of *amon* protein is sufficient to rescue the $amon^{C241Y}$ mutant allele (Figure 6) indicate that this complementation group corresponds to *amon*. Three *amon* mutations

TABLE 3

Lethal phase analysis of *amon* mutants

	% survival				
Genotype	36 hr	60 hr	96 hr	120 hr	Adult
E601sa	37	9	0	—	—
G367V	62	20	0	—	—
G473R	50	42	2	0	—
C254Y	84	38	2	0	—
Q178st	74	54	4	0	—
S557L	62	25	5	0	—
C241Y	66	34	8	0	—
Q507sa	58	32	6	2	—
red e	90	70	68	66	60

amon mutants heterozygous to the *Df(3R)Tl-X* deficiency chromosome, recognizable by the absence of the GFP marker, were scored for survival at the following times: 36 hr ae1, 60 hr ae1, 96 hr ae1, and 120 hr ae1. In wild-type animals, these times correlate to the approximate midpoints of first, second, and third larval instars and to pupariation, respectively. Percentage of survival is expressed as the percentage of non-GFP animals expected (50 animals) from a collection of 200 eggs (see MATERIALS AND METHODS). The percentage of survival given for S557L represents the average of values determined for $amon^{S557L1}$ and $amon^{S557L2}$.

($amon^{Q178st}$, $amon^{Q507sa}$, and $amon^{E601sa}$) are predicted to result in truncation of the *amon* protein due to premature stop codons or improper RNA splicing. The remaining six *amon* mutations are missense mutations that affect residues essential for *amon* function. Four of these mutations ($amon^{C241Y}$, $amon^{C254Y}$, $amon^{G367V}$, and $amon^{G473R}$) affect residues highly conserved within the kexin subfamily of the subtilisin-like serine proteases (SIEZEN and LEUNISSEN 1997) while the other two mutations ($amon^{S557L1}$ and $amon^{S557L2}$) reveal a residue within the P domain that is critical for AMON activity.

The other complementation group identified here, *doc*, consists of three lethal mutations and one recessive viable mutation that affects distal wing derivatives (Figure 2). Comparison of the genetic map shown in Figure 1 to the annotated Drosophila genome sequence (FLYBASE 2002) yields centromere proximal and distal limits for annotated genes that may correspond to *doc*. A proximal limit is provided by the *scribbled* (*scrib*) gene, which maps within *Df(3R)Tl-X* but proximal to *Df(3R)ro80b* (KIDD *et al.* 1999). A distal limit is provided by the *Toll* gene, which is disrupted by the distal endpoint of *Df(3R)Tl-X* (ANDERSON *et al.* 1985). Within this interval of ~200 kb are 10 genes whose predictions are supported by cDNA evidence (FLYBASE 2002). Seven of these predicted genes are centromere proximal to *amon* and the remaining three genes lie between *amon* and *Toll*. Determination of the position of the proximal endpoint of *Df(3R)ro80b* within the genome sequence will provide a closer proximal limit and may narrow this interval considerably. In addition, determination of the relative proximal-distal order of *amon* and *doc* within the overlap of *Df(3R)Tl-X* and *Df(3R)ro80b* will be helpful in assigning the *doc* complementation group to an annotated gene.

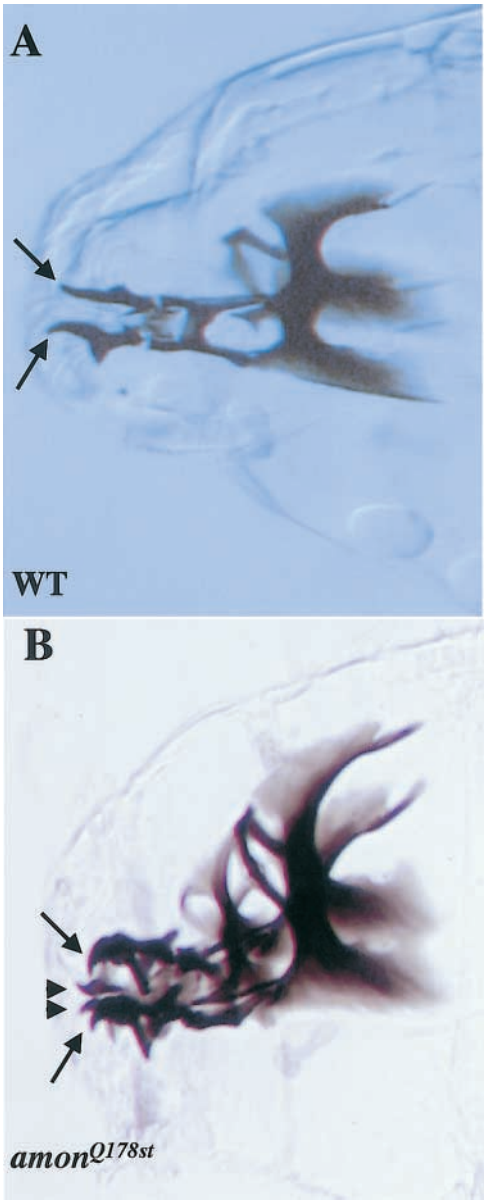

FIGURE 5.—*amon* mutants are defective in molting. (A) A wild-type sibling [*Df(3R)Tl-X/TM6B GFP Tb*] second instar larva shows normal mouth hook formation. Second instar mouth hooks are indicated by arrows. (B) An *amon* mutant [$amon^{Q178st}$/*Df(3R)Tl-X*] larva arrested during the first larval instar. Second instar mouth hooks are indicated by arrows and first instar mouth hooks are indicated by arrowheads.

***amon* mutants display early developmental phenotypes:** Hemizygous *amon* point mutants die during early development. All *amon* mutants exhibit some degree of embryonic lethality and most *amon* mutants die within 96 hr after egg laying (Table 3). At times corresponding to mid-second and mid-third instar larval stages in wild-type animals, *amon* mutants are dramatically smaller

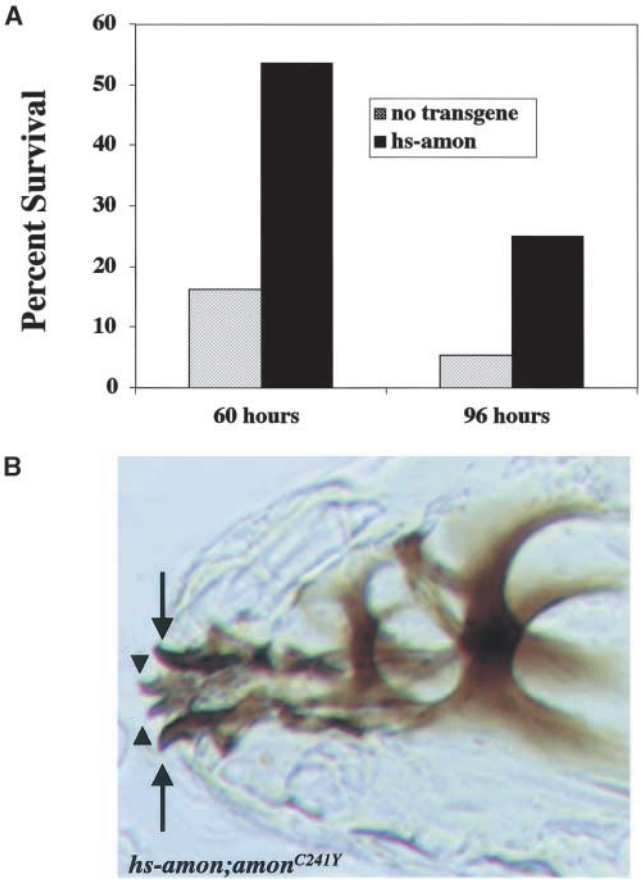

FIGURE 6.—Rescue of *amon* mutants. (A) Hemizygous *amon* mutants carrying an *hs-amon* transgene on the second chromosome [*yw; hs-amon/+; amon*^{C241Y}*/Df(3R)Tl-X*] were scored for survival at 60 and 96 hr ael (solid bars). After egg collection (n = 200 eggs), animals were heat-shocked for 30 min at 37° every 12 hr starting at 36 hr ael. Control animals hemizygous for *amon* but lacking the transgene [*yw; amon*^{C241Y}*/Df(3R)Tl-X*] were treated in the same way (shaded bars). Percentage of survival was calculated by dividing the number of surviving *amon* mutants (marked by *yellow*) by the number of *amon* mutants expected (50% of non-*yellow* siblings). (B) An *amon* mutant carrying the transgene arrested at the 96-hr time point has second (arrowheads) and third (arrows) instar larval mouth hooks, indicating rescue beyond the first to second instar larval molt arrest observed in *amon* mutants lacking the transgene.

than control larvae, suggesting that larval growth is delayed or blocked in *amon* mutants. The majority of arrested *amon* mutants exhibit duplicated larval mouthparts (Figure 5), indicating that *amon* mutants arrest during the first to second instar larval molt. The presence of both first and second instar larval mouthparts suggests that *amon* mutants complete early stages of the molting cycle, including apolysis of the first instar cuticle and formation of second instar derivatives, but are incapable of undergoing ecdysis to shed the first instar larval cuticle. Heat-shock-controlled expression of *amon* protein from a transgene is sufficient to rescue both growth and larval molting (Figure 6) defects exhibited by *amon* mutants. In a few cases, *amon* mutants were rescued to adult eclosion, although most rescued animals died during late larval or early pupal development. Animals that arrest during late larval development exhibited both second and third instar larval mouthparts, suggesting that *amon* is also required for the second to third instar larval molt.

A previous study concluded that *amon* is required for a hatching behavior consisting of a series of head-swinging episodes in which the larva scrapes its mouthhooks against the anterior portion of the eggshell prior to hatching (SIEKHAUS and FULLER 1999). This study showed that animals heterozygous for two overlapping deficiencies [*Df(3R)Tl-X/Df(3R)ro80b*] fail to hatch from the egg and are defective for hatching behavior. *Df(3R)Tl-X/Df(3R)ro80b* animals are deficient for *amon* and flanking genes. Hatching behavior can be rescued in *Df(3R)Tl-X/Df(3R)ro80b* animals by heat-shock-induced expression of *amon*, indicating that *amon* is required for the hatching behavior described. However, *amon*'s role in hatching itself could not be assessed in these experiments since *Df(3R)Tl-X/Df(3R)ro80b* animals lack not only *amon* but also *Toll*, *doc*, and at least two and up to nine other genes predicted by EST evidence (FLYBASE 2002). While we have not directly analyzed the hatching behavior of the *amon* mutants, the embryonic lethality of each of the nine point mutants indicates that *amon* contributes to but is not absolutely required for hatching from the egg. Thus, each of the *amon* point mutants described here displays some degree of embryonic lethality but none is completely defective in hatching (Table 3). These results suggest that multiple behavioral pathways may be integrated to control successful hatching from the egg. If so, this situation would be analogous to adult eclosion in insects, where the peptide eclosion hormone is sufficient to initiate eclosion (reviewed in HORODYSKI 1996) but is not strictly required for ecdysis (MCNABB *et al.* 1997).

Potential targets for AMON activity: Ultimately, we want to identify the AMON substrates that are responsible for the larval growth and molting defects exhibited by *amon* mutants. The high degree of homology between AMON and the vertebrate PC2 prohormone convertase and the expression of *amon* in cells of the brain and ventral nerve cord (SIEKHAUS and FULLER 1999) suggest that AMON functions as a prohormone processing protease within neural cells in Drosophila. This conclusion is supported by rescue experiments in which mutation of one of the three predicted catalytic residues of AMON strongly reduces rescue of hatching behavior compared to the wild-type *amon* protein (SIEKHAUS and FULLER 1999).

One aspect of the *amon* mutant phenotype is delayed growth during larval development. Loss of vertebrate PC2 in the mouse results in defects in proinsulin and proglucagon processing and alterations in normal carbohydrate metabolism (FURUTA *et al.* 1997, 1998). The

insulin signaling pathway is remarkably well conserved in Drosophila (reviewed in Garofalo 2002). Drosophila has seven insulin-like peptides (*dilp* 1–7), five of which are significantly homologous to human and mouse insulin. A recent study (Rulifson *et al.* 2002) has shown that ablation of the brain insulin-producing cells (IPCs) in Drosophila results in severe growth defects and developmental delays. Larvae with ablated IPCs reached only 58% of the normal size and took 12 days to develop to the puparium stage, a process that normally takes only 5 days. These phenotypes are intriguing because the *amon* mutants also consistently appeared smaller than their wild-type siblings during our lethal phase analysis. We speculate that *amon* may influence insulin signaling in Drosophila, perhaps by proteolytically processing and activating insulin-like peptides.

amon mutants are also defective in larval molting. Larval molting is a highly regulated process involving interactions among the steroid hormone ecdysone and the peptide hormones eclosion hormone (EH), ecdysis-triggering hormone (ETH), and crustacean cardioactive peptide (CCAP; reviewed in Mesce and Fahrbach 2002). A drop in ecdysone titer is required to trigger ecdysis in insects. Furthermore, mutations that inactivate the EcR subunit of the ecdysone receptor in Drosophila arrest during larval ecdysis with duplicated larval mouthparts (Schubiger *et al.* 1998; Li and Bender 2000), a phenotype identical to that described here for *amon*. Ecdysis itself is coordinated by the peptide hormones EH, ETH, and CCAP. EH and ETH act in a positive feedback loop in which low levels of circulating ETH trigger the release of EH from the brain, which induces exhaustive release of ETH from the Inka cells and EH from the brain (Ewer *et al.* 1997; Zitnan *et al.* 1999). Studies in the moth, *Manduca sexta*, have demonstrated that EH acts through a second messenger system to cause elevated levels of cGMP in CCAP-expressing cells (Ewer *et al.* 1997). CCAP release elicits ecdysis motor bursts while suppressing the pre-ecdysis behaviors initiated by EH (Gammie and Truman 1997). Thus CCAP appears to serve as the proximate trigger for ecdysis.

The EH, ETH, and CCAP genes have all been identified in Drosophila. All three peptides contain potential dibasic endoproteolytic cleavage sites (Horodyski *et al.* 1993; Park *et al.* 1999; Loi *et al.* 2001), thus making them potential AMON substrates. Targeted ablation of EH-producing cells results in disruption of larval and adult ecdysis, although disruption is not complete as approximately one-third of targeted animals emerge as adults with specific behavioral defects (McNabb *et al.* 1997). Inactivation of *eth* results in blockage of ecdysis behaviors and nearly complete arrest during larval molting (Park *et al.* 2002). Arrested *eth* mutants also exhibit duplicated larval mouthparts, indicating that loss of either *amon* or *eth* results in arrest at a similar stage during the larval molting cycle. These results are consistent with the hypothesis that the *amon* protein acts to proteolytically process neuropeptide hormones that function to trigger larval ecdysis in Drosophila. Further experiments, including colocalization of AMON and potential neuropeptide targets and direct biochemical assay of AMON activity, will be required to establish a direct link between AMON and candidate neuropeptide hormone targets.

It is notable that mutants in another peptide hormone processing enzyzme, PHM, also die during late embryogenesis and early larval development and exhibit defects in larval molting similar to those described here for *amon* (Jiang *et al.* 2000). PHM acts to α-amidate C-terminal residues of secretory peptides, a modification often required for normal activity of the peptide. By conditional rescue of PHM mutants via heat-shock-controlled PHM expression, Jiang *et al.* (2000) have also shown that PHM is required for later development including puparium formation and completion of adult development. These results suggest that amidated secretory peptides are required during multiple developmental transitions during the Drosophila life cycle. Does AMON similarly act to process neuropeptide hormones throughout the life cycle? It is interesting to note that, in addition to its embryonic expression, *amon* expression is detectable during larval and pupal development, increases in late pupae, and peaks during the adult stage (Siekhaus and Fuller 1999). Conditional rescue of *amon* mutants by heat-shock-induced AMON expression, currently in progress (L. Y. M. Rayburn, S. Jocoy and M. Bender, unpublished data), should allow investigation of *amon* requirements during pupal development and in the adult.

We thank Dr. Kathryn Anderson for providing Drosophila stocks and David Brown, Jennifer Keyes, Don Latner, and Anne Robertson for expert technical assistance. We also acknowledge two reviewers for comments that improved the manuscript. This work was supported by a grant from the National Institutes of Health (NIH; GM-53681) to M.B., by an NIH training grant (GM-07103) to L.Y.M.R., and by a summer undergraduate research fellowship from the Howard Hughes Medical Institute and a Barry M. Goldwater undergraduate scholarship to D.M.

LITERATURE CITED

Adams, M. D., S. E. Celniker, R. A. Holt, C. A. Evans, J. D. Gocayne *et al.*, 2000 The genome sequence of Drosophila melanogaster. Science **287:** 2185–2195.

Anderson, K. V., G. Jurgens and C. Nusslein-Volhard, 1985 Establishment of dorsal-ventral polarity in the Drosophila embryo: genetic studies on the role of the Toll gene product. Cell **42:** 779–789.

Benjannet, S., N. Rondeau, R. Day, M. Chretien and N. G. Seidah, 1991 PC1 and PC2 are proprotein convertases capable of cleaving proopiomelanocortin at distinct pairs of basic residues. Proc. Natl. Acad. Sci. USA **88:** 3564–3568.

Bergeron, F., R. Leduc and R. Day, 2000 Subtilase-like pro-protein convertases: from molecular specificity to therapeutic applications. J. Mol. Endocrinol. **24:** 1–22.

Brar, B. K., and P. J. Lowry, 1999 The differential processing of proenkephalin A in mouse and human breast tumour cell lines. J. Endocrinol. **161:** 475–484.

Bryan, P., M. W. Pantoliano, S. G. Quill, H.-Y. Hsiao and T. Poulos, 1986 Site-directed mutagenesis and the role of the oxyanion hole in subtilisin. Proc. Natl. Acad. Sci. USA **83:** 3743–3745.

Creemers, J. W., R. S. Jackson and J. C. Hutton, 1998 Molecular and cellular regulation of prohormone processing. Semin. Cell Dev. Biol. **9:** 3–10.

Ewer, J., S. C. Gammie and J. Truman, 1997 Control of insect ecdysis by a positive-feedback endocrine system: roles of eclosion hormone and ecdysis triggering hormone. J. Exp. Biol. **200:** 869–881.

FlyBase, 2002 The FlyBase database of the Drosophila genome projects and community literature. Nucleic Acids Res. **30:** 106–108.

Furuta, M., H. Yano, A. Zhou, Y. Rouille, J. J. Holst *et al.*, 1997 Defective prohormone processing and altered pancreatic islet morphology in mice lacking active SPC2. Proc. Natl. Acad. Sci. USA **94:** 6646–6651.

Furuta, M., R. Carroll, S. Martin, H. H. Swift, M. Ravazzola *et al.*, 1998 Incomplete processing of proinsulin to insulin accompanied by elevation of Des-31,32 proinsulin intermediates in islets of mice lacking active PC2. J. Biol. Chem. **273:** 3431–3437.

Gammie, S. C., and J. W. Truman, 1997 Neuropeptide hierarchies and the activation of sequential motor behaviors in the hawkmoth, Manduca sexta. J. Neurosci. **17:** 4389–4397.

Garofalo, R. S., 2002 Genetic analysis of insulin signaling in Drosophila. Trends Endocrinol. Metab. **13:** 156–162.

Horodyski, F., 1996 Neuroendocrine control of insect ecdysis by eclosion hormone. J. Insect. Physiol. **42:** 917–924.

Horodyski, F. M., J. Ewer, L. M. Riddiford and J. W. Truman, 1993 Isolation, characterization and expression of the eclosion hormone gene of Drosophila melanogaster. Eur. J. Biochem. **215:** 221–228.

Hwang, J. R., D. E. Siekhaus, R. S. Fuller, P. H. Taghert and I. Lindberg, 2000 Interaction of Drosophila melanogaster prohormone convertase 2 and 7B2. Insect cell-specific processing and secretion. J. Biol. Chem. **275:** 17886–17893.

Jiang, N., A. S. Kolhekar, P. S. Jacobs, R. E. Mains, B. A. Eipper *et al.*, 2000 PHM is required for normal developmental transitions and for biosynthesis of secretory peptides in Drosophila. Dev. Biol. **226:** 118–136.

Kidd, A. R., III, D. Tolla and M. Bender, 1999 New lethal mutations in the 97B1–10 to 97D13 region of the *Drosophila melanogaster* 3rd chromosome. Dros. Inf. Serv. **82:** 114–115.

Lewis, E. B., and F. Bacher, 1968 Method of feeding ethyl methane sulfonate (EMS) to Drosophila males. Dros. Inf. Serv. **43:** 193.

Li, T., and M. Bender, 2000 A conditional rescue system reveals essential functions for the ecdysone receptor (EcR) gene during molting and metamorphosis in Drosophila. Development **127:** 2897–2905.

Lindsley, D. L., and G. G. Zimm, 1992 *The Genome of Drosophila melanogaster.* Academic Press, San Diego.

Lipkind, G. M., A. Zhou and D. F. Steiner, 1998 A model for the structure of the P domains in the subtilisin-like prohormone convertases. Proc. Natl. Acad. Sci. USA **95:** 7310–7315.

Loi, P. K., S. A. Emmal, Y. Park and N. J. Tublitz, 2001 Identification, sequence and expression of a crustacean cardioactive peptide (CCAP) gene in the moth Manduca sexta. J. Exp. Biol. **204:** 2803–2816.

McNabb, S. L., J. D. Baker, J. Agapite, H. Steller, L. M. Riddiford *et al.*, 1997 Disruption of a behavioral sequence by targeted death of peptidergic neurons in Drosophila. Neuron **19:** 813–823.

Mesce, K. A., and S. E. Fahrbach, 2002 Integration of endocrine signals that regulate insect ecdysis. Front. Neuroendocrinol. **23:** 179–199.

Muller, L., and I. Lindberg, 2000 The cell biology of the prohormone convertases PC1 and PC2. Progr. Nucleic Acid Res. Mol. Biol. **63:** 69–108.

Park, Y., D. Zitnan, S. S. Gill and M. E. Adams, 1999 Molecular cloning and biological activity of ecdysis-triggering hormones in *Drosophila melanogaster.* FEBS Lett. **463:** 133–138.

Park, Y., V. Filippov, S. S. Gill and M. E. Adams, 2002 Deletion of the ecdysis-triggering hormone gene leads to lethal ecdysis deficiency. Development **129:** 493–503.

Rayburn, L. Y. M., S. P. Choksi and M. Bender, 2002 Correction of an *amontillado* (*amon*) cDNA artifact and identification of single nucleotide polymorphisms in the *amon* gene. Dros. Inf. Serv. (in press).

Rockwell, N. C., G. T. Wang, G. A. Krafft and R. S. Fuller, 1997 Internally consistent libraries of fluorogenic substrates demonstrate that Kex2 protease specificity is generated by multiple mechanisms. Biochemistry **36:** 1912–1917.

Rouille, Y., G. Westermark, S. K. Martin and D. F. Steiner, 1994 Proglucagon is processed to glucagon by prohormone convertase PC2 in alpha TC1–6 cells. Proc. Natl. Acad. Sci. USA **91:** 3242–3246.

Rouille, Y., S. J. Duguay, K. Lund, M. Furuta, Q. Gong *et al.*, 1995a Proteolytic processing mechanisms in the biosynthesis of neuroendocrine peptides: the subtilisin-like proprotein convertases. Front. Neuroendocrinol. **16:** 322–361.

Rouille, Y., S. Martin and D. F. Steiner, 1995b Differential processing of proglucagon by the subtilisin-like prohormone convertases PC2 and PC3 to generate either glucagon or glucagon-like peptide. J. Biol. Chem. **270:** 26488–26496.

Rulifson, E. J., S. K. Kim and R. Nusse, 2002 Ablation of insulin-producing neurons in flies: growth and diabetic phenotypes. Science **296:** 1118–1120.

Schubiger, M., A. A. Wade, G. E. Carney, J. W. Truman and M. Bender, 1998 Drosophila EcR-B ecdysone receptor isoforms are required for larval molting and for neuron remodeling during metamorphosis. Development **125:** 2053–2062.

Seidah, N. G., S. Benjannet, J. Hamelin, A. M. Mamarbachi, A. Basak *et al.*, 1999 The subtilisin/kexin family of precursor convertases. Emphasis on PC1, PC2/7B2, POMC and the novel enzyme SKI-1. Ann. NY Acad. Sci. **885:** 57–74.

Shennan, K. I., S. P. Smeekens, D. F. Steiner and K. Docherty, 1991 Characterization of PC2, a mammalian Kex2 homologue, following expression of the cDNA in microinjected Xenopus oocytes. FEBS Lett. **284:** 277–280.

Siekhaus, D. E., and R. S. Fuller, 1999 A role for amontillado, the Drosophila homolog of the neuropeptide precursor processing protease PC2, in triggering hatching behavior. J. Neurosci. **19:** 6942–6954.

Siezen, R. J., and J. A. Leunissen, 1997 Subtilases: the superfamily of subtilisin-like serine proteases. Protein Sci. **6:** 501–523.

Smeekens, S. P., A. S. Avruch, J. LaMendola, S. J. Chan and D. F. Steiner, 1991 Identification of a cDNA encoding a second putative prohormone convertase related to PC2 in AtT20 cells and islets of Langerhans. Proc. Natl. Acad. Sci. USA **88:** 340–344.

Sossin, W. S., J. M. Fisher and R. H. Scheller, 1989 Cellular and molecular biology of neuropeptide processing and packaging. Neuron **2:** 1407–1417.

Steiner, D. F., Y. Rouille, Q. Gong, S. Martin, R. Carroll *et al.*, 1996 The role of prohormone convertases in insulin biosynthesis: evidence for inherited defects in their action in man and experimental animals. Diabetes Metab. **22:** 94–104.

Yoshida, H., S. Ohagi, T. Sanke, H. Furuta, M. Furuta *et al.*, 1995 Association of the prohormone convertase 2 gene (*PCSK2*) on chromosome 20 with NIDDM in Japanese subjects. Diabetes **44:** 389–393.

Zhou, A., S. Martin, G. Lipkind, J. LaMendola and D. F. Steiner, 1998 Regulatory roles of the P domain of the subtilisin-like prohormone convertases. J. Biol. Chem. **273:** 11107–11114.

Zhou, A., G. Webb, X. Zhu and D. F. Steiner, 1999 Proteolytic processing in the secretory pathway. J. Biol. Chem. **274:** 20745–20748.

Zhu, X. L., Y. Ohta, F. Jordan and M. Inouye, 1989 Pro-sequence of subtilisin can guide the refolding of denatured subtilisin in an intermolecular process. Nature **339:** 483–484.

Zitnan, D., L. S. Ross, I. Zitnanova, J. J. Hermesman, S. S. Gill *et al.*, 1999 Steroid induction of a peptide hormone gene leads to orchestration of a defined behavioral sequence. Neuron **23:** 523–535.

Communicating editor: A. J. Lopez